



Published in final edited form as:

*J Cell Mol Med.* 2014 April ; 18(4): 685–697. doi:10.1111/jcmm.12217.

## Nanofiber-expanded human umbilical cord blood-derived CD34<sup>+</sup> cell therapy accelerates cutaneous wound closure in NOD/SCID mice

Suman Kanji, Manjusri Das, Reeva Aggarwal, Jingwei Lu, Matthew Joseph, Vincent J. Pompili, and Hiranmoy Das\*

Stem Cell Research Laboratory, Cardiovascular Medicine, Davis Heart and Lung Research Institute, Wexner Medical Center at The Ohio State University, Columbus, Ohio 43210

### Abstract

Nanofiber-expanded human umbilical cord blood-derived CD34<sup>+</sup> cell therapy has been shown to have potential applications for peripheral and myocardial ischemic diseases. However, the efficacies of expanded CD34<sup>+</sup> cell therapy for treating cutaneous wounds and its mechanisms of action have yet to be established. Using an excisional wound model in NOD/SCID mice, we show herein that CD34<sup>+</sup> cells accelerate the wound-healing process by enhancing collagen synthesis, and increasing fibroblast cell migration within the wound bed. Concomitantly, reduced levels of matrix metalloproteinase (MMPs) such as MMP1, MMP3, MMP9 and MMP13 were detected found in the wound beds of animals treated with CD34<sup>+</sup> cells compared to vehicle-treated controls. CD34<sup>+</sup> cells were found to mediate enhanced migration and proliferation of dermal fibroblast cells *in vitro*. Moreover, CD34<sup>+</sup> cells secrete collagen in a serum-deprived environment. In mechanistic studies, co-culture of CD34<sup>+</sup> cells with primary skin fibroblasts increased the expression of collagen1A1, a component of type 1 collagen, and decreased the expression of MMP1 in fibroblast cells in the presence of a proteasome inhibitor. Finally, CD34<sup>+</sup> cell-mediated functions were transcriptionally regulated by the JNK pathway. Collectively, these data provide evidence of therapeutic efficacy and a novel mechanism of nanofiber-expanded CD34<sup>+</sup> cell-mediated accelerated wound healing.

### Keywords

Human umbilical cord blood; nanofiber-expanded CD34<sup>+</sup> cells; cutaneous wound; NOD/SCID mice; collagen; MMPs

### Introduction

Wound healing is a complex biological process, requiring the involvement of various cell types and their mediators in an orchestrated manner, and characterized by an acute inflammatory phase followed by extracellular matrix (ECM) remodeling [1,2]. Fibroblasts are the most important cells producing collagen-based ECM, which replaces the fibrin-based provisional matrix, and facilitate re-approximation of wound edges through their contractile properties as they migrate into the affected area [3]. Thus, the processes of fibroblast

\*Address correspondence to: Hiranmoy Das, PhD, Associate Professor of Internal Medicine, Director, Cardiovascular Stem Cell Laboratories, The Dorothy M. Davis Heart and Lung Research Institute, Wexner Medical Center at The Ohio State University, 460 W. 12th Avenue, BRT 382, Columbus, Ohio 43210, (614) 688-8711 office, (614) 293-5614 fax, hiranmoy.das@osumc.edu.

### Author disclosure statement

No competing financial interests exist

migration, proliferation, and ECM production within the wound bed are key steps in regeneration of functional dermis [4]. As healing progresses, fibroblasts differentiate into myofibroblasts to promote wound contraction [3,4]. In addition to coordinating processes, such as ECM synthesis, cell to cell interaction, and cell to cytokine interactions, dermal fibroblasts not only repair wounds but also maintain the integrity of the skin [3,4]. Any malfunction of the orchestrated cascades, such as impaired migration and proliferation of fibroblasts, will compromise the deposition of ECM and will result in delayed or impaired wound closure.

Matrix-metalloproteinases (MMPs), such as MMP-1, -2, and -3 are the enzymes responsible for degradation and turnover of ECM, and spatio-temporal regulation of MMPs is critical for effective wound healing. MMPs are also involved in tissue repair and remodeling processes such as inflammation, re-epithelialization, and angiogenesis [5]. An imbalance in activity of MMPs is often associated with chronically impaired wound healing [6]. Production of MMPs is transcriptionally regulated, and requires activation from inactive precursors (proMMP) [7]. MMP-1 cleaves type I collagen by unwinding their triple helix chains to make them susceptible to further degradation [8]. In normal wound healing MMP3 helps in epithelial cell migration, whereas MMP9 promotes inflammation and facilitates the migration of neutrophils, and MMP13 mediates endothelial cell migration. However, in the chronic wound, the levels of these MMPs are elevated [9,10]. The activity of MMPs also depends on their interactions with ECM components and binding to endogenous inhibitors, such as tissue inhibitor of metalloproteinases (TIMP) [11].

Type I collagen is an important ECM components of the skin required for normal growth, differentiation, and wound repair [12]. Collagen-I enhances ECM cross-linking, resulted in increased mechanical strength in the wound. Type I collagen forms a triple-helix structure composed of two alpha 1 subunits and one alpha 2 subunit, encoded by the collagen 1A1 (COL1A1) and COL1A2 genes. Tightly regulated synthesis of these two moieties ensures a 2:1 ratio of COL1A1 and COL1A2 [13].

Despite advances in wound care, cutaneous wound healing often demands significant long-term medical attention, and is responsible for huge expenses [14]. Available medical interventions, such as systemic (e.g. hyperbaric oxygen therapy) or topical (e.g. growth factor; PDGF) therapy, and mechanical devices for wound protection, often fail to cure cutaneous wounds, leading to a significant number of peripheral amputations. Stem cells have long been recognized for their regenerative properties and viewed as potential therapeutics for healing wounds [15–17]. The number of CD34<sup>+</sup> stem cells obtained from a single cord is not sufficient for any preclinical or clinical application. Therefore, variety methods have been adopted, by which cord blood-derived stem cells can be expanded many fold without compromising their phenotype and stem cell characteristics.

Previously, we have shown that the human umbilical cord blood-derived CD34<sup>+</sup> cells can be expanded efficiently (almost 250- fold) on aminated nanofibers while preserving their stemness. In addition, after nanofiber expansion CD34<sup>+</sup> cells constitutively express high levels of a pro-migratory surface molecule (CXCR4), which helps them to mobilize to the challenged area. These umbilical cord blood-derived nanofiber expanded CD34<sup>+</sup> cells also show biological functionality in regenerating tissues in hind limb ischemia and myocardial infarction models [18,19]. However, both the efficacy of nanofiber-expanded CD34<sup>+</sup> cells in cutaneous wound healing and their mechanisms of action have yet to be demonstrated.

In this current study, using an excisional wound model in NOD/SCID mice, we show that CD34<sup>+</sup> cells accelerate wound closure by enhancing collagen synthesis, and increasing fibroblast cell migration within the wound bed. CD34<sup>+</sup> cell therapy mediated accelerated

wound closure was associated with reduced levels of MMPs. Accelerated wound closure might also be facilitated by enhanced ECM formation in the form of CD34<sup>+</sup> cell mediated secretion of collagen. Moreover, co-culture studies using primary dermal fibroblast cells indicate that the ability of CD34<sup>+</sup> cells to enhance fibroblast migration, increase expression of collagen1A1 and decrease expression of MMP1 in dermal fibroblasts is mediated through the JNK pathway. Collectively, these data provide evidence for therapeutic efficacy and a novel mechanism of nanofiber-expanded CD34<sup>+</sup> cell-mediated accelerated wound healing.

## Materials and methods

### CD133<sup>+</sup> cell isolation

Human umbilical cord blood was freshly collected from The Wexner Medical Center at The Ohio State University after IRB approval, following written consent from donors, and was processed according to the protocol described earlier [18]. Briefly, after gradient separation by the Ficoll centrifugation method, CD133<sup>+</sup> cells were isolated using an AutoMACS device (Miltenyi Biotec, Auburn, CA), and the purity of the isolated cells as well as phenotypes after expansion were determined by flowcytometry [18].

### Ex-vivo expansion of isolated cells

Freshly isolated CD133<sup>+</sup> cells, which also co-express the CD34 molecule were expanded by following the previously described protocol [18]. Briefly, eight hundred CD133<sup>+</sup> cells were cultured in a well of a 24-well plate coated with nanofiber mesh (a kind gift from Hai-Quan Mao, PhD, Johns Hopkins University, Baltimore, MD) in 600  $\mu$ l of StemSpan SFEM, a serum-free expansion medium (Stem Cell Technologies, Vancouver, BC, Canada) containing essential supplements. Cells were cultured at 37 °C in an atmosphere containing 5% CO<sub>2</sub> without changing culture medium, and harvested after 10 days. Before experiments, flow cytometry was performed to characterize the expanded cells. The majority of the expanded cells loses CD133 expression and retains CD34 expression.

### GFP labeling of CD34<sup>+</sup> cells

Nanofiber-expanded cord blood derived CD34<sup>+</sup> cells were transfected with GFP containing vector (pmaxGFP) using the human CD34 cell specific Nucleofector kit (Amaxa Inc.), following the manufacturer's protocol. After transfection, cells were cultured overnight in a serum-free complete medium and transplanted into the experimental mice.

### Fibroblast cell culture

A primary human dermal fibroblast cell line was established from skin punch biopsies of a healthy donor. Primary human dermal fibroblast cells (a generous gift from Dr. Heather M. Powell, Department of Materials Science and Engineering, Department of Biomedical Engineering, The Ohio State University, Columbus, Ohio) were maintained in Dulbecco's modified Eagle's medium (DMEM) (Invitrogen Corporation, Carlsbad, CA, USA).

DMEM medium was supplemented with 4% fetal calf serum (FCS) (Sigma-Aldrich, St. Louis, MO, USA), 2 mM glutamine (Invitrogen Corporation), 5  $\mu$ g/ml insulin (Sigma-Aldrich, St. Louis, MO, USA), 0.5  $\mu$ g/ml hydrocortisone (Sigma-Aldrich, St. Louis, MO, USA), 0.1 mM ascorbic acid-2-phosphate (Sigma-Aldrich, St. Louis, MO, USA), 50 U/ml penicillin, and 50  $\mu$ g/ml streptomycin (Invitrogen Corporation), grown in 5% CO<sub>2</sub> at 37°C, and were used within passages 3 to 6.

### Full thickness excisional cutaneous wound model

All animal experiments were performed according to the protocols approved by the Institutional Animal Care and Use Committee (IACUC) of The Ohio State University, Columbus, OH. Six to eight week old male nonobese diabetic/severe combined immune deficient (NOD/SCID) mice were used for this study and were purchased from Jackson Laboratory (Bar Harbor, ME). Prior to generating a cutaneous wound, the mouse was anesthetized, the dorsum was clipped, hair was removed, and the area was wiped with Betadine solution. A full-thickness wound was made on the dorsal skin in each mouse using 8 mm skin punch biopsy (Acuderm Inc. Fort Lauderdale, FL).

### Transplantation of nanofiber-expanded GFP-labeled or unlabeled CD34<sup>+</sup> cells

Ten-day nanofiber-expanded CD34<sup>+</sup> cells ( $0.5 \times 10^6$  cells/mouse) or GFP transfected (24 hours prior to injection) CD34<sup>+</sup> cells ( $0.5 \times 10^6$  cells/mouse) in a 200  $\mu$ l volume of serum-free DMEM media was injected into each mouse (n=15), and media alone was injected as a control (n=15) through lateral tail vein 2 hrs of post wounding. Three mice were harvested from each group at days 3, 5, and 7. At each time point skin samples (wound and 2 mm of the surrounding skin) were harvested, and part of the sample was snap frozen in liquid nitrogen while the other part was formalin fixed for further evaluations.

### Evaluation of wound area

Photographic images of wounds were taken on days 0, and 3, 5, and 7 after generation of wound using a digital camera (Sony cyber-shot DSC-H10) from a fixed distance. Wound closure rate was measured by tracing the wound area onto a sheet of acetate paper on each day stated above following an earlier published method [20]. The wound impressions were scanned and digitalized, and the areas were measured by using the UTHSCSA (University of Texas Health Science Center at San Antonio) image tool (Version 3.00) and converted to percent wound. The percentage of wound closure was calculated as follows: (Area of wound on day 0 - Area of wound on day of examination)/Area of wound on day 0  $\times$  100). The investigators measuring samples were blinded.

### Immunohistochemistry

Mice were sacrificed at various time points (days 3, 5, and 7) of the experiments, and skin tissues were harvested so that part of the tissue was fixed in formalin-PBS buffer, paraffin-embedded, and sectioned to generate wound-edge specimens of 4  $\mu$ m diameter. After deparaffinized, sections were stained with Masson's trichrome by standard procedures and examined under light microscopy. For immunofluorescence staining, antigen retrieval was performed using citrate buffer, pH to 6.0, and microwaving for 5 min then cooling for 3 min. After non-specific blocking, specific staining was performed by using  $\alpha$ -SMA (Sigma-Aldrich, St. Louis, MO, USA), Pro-collagen 1A1 (Santa Cruz, CA) Ab, or SM22 $\alpha$  (Abcam, USA) Ab followed by incubation with secondary antibody alexa fluor 594-conjugated IgG or Texas red (Invitrogen, Molecular Probe, Carlsbad, CA). Counterstaining was performed with DAPI (Invitrogen) and imaged by using a fluorescent microscope (Nikon E800 with MetaMorph version 4.5 software, Universal Imaging Corp.). The GFP staining procedure was carried out according to the protocol of VECTASTAIN Elite ABC kit (Vector laboratories Inc, Burlingame, CA) after using anti- GFP primary antibody (Zymed, Invitrogen). Immunohistochemical images were analyzed using an image analysis software program (ImageJ, NIH).

### Fibroblast cell proliferation assay

The fibroblast cell proliferation assay was performed in a two-chambered 24-well plate. Human primary dermal fibroblasts (passage between 3–6) were seeded at  $3 \times 10^3$  cells/well in

the lower chamber of a 24-well plate in DMEM complete media (10% FBS) and allowed to adhere, then starved overnight in DMEM (1% FBS) media. After serum starvation,  $5 \times 10^5$  CD34<sup>+</sup> cells were added to the upper chamber in DMEM media containing 1% FBS and inserted into the fibroblast culture. Similar media without cells was inserted in a separate well as a control. After co-culture of the fibroblast and CD34<sup>+</sup> cells for 48 h, the upper chambers were removed; fibroblast cells were trypsinized and counted with the trypan blue exclusion method using a Vicell Cell Viability Analyzer. Fibroblast cell culture media was also frozen at  $-20^\circ\text{C}$  for soluble collagen estimation later using a Sircol collagen assay kit.

### Scratch wound closure assay

The *In vitro* wound closure assay was performed in the lower chamber of a twochambered 24-well plate using human dermal fibroblasts. Confluent human dermal fibroblasts were cultured in serum-deprived (1% FBS) DMEM for 24 h in the lower chamber of a 24-well plate, then wounded with a plastic micropipette tip having a large orifice. Scratched wells were washed with media to remove cell debris, and then either an empty control insert containing DMEM (1% FBS) media or CD34<sup>+</sup> cells ( $5 \times 10^5$  cells/well) DMEM (1% FBS) media containing insert was placed in the scratched fibroblast well. Photographs of scratched areas were taken at 0 h and 48 h under a phase-contrast microscope. Wound closure was assessed by quantifying the number of fibroblasts migrated to the scratched region [21].

### Quantitative RT-PCR analysis

A quarter of a million fibroblast cells were seeded in a well of a 6-well plate, and serumstarved overnight. Then, either the proteasome inhibitor, MG132 (10  $\mu\text{M}$ ), medium alone, CD34<sup>+</sup> ( $0.25 \times 10^6$ ) cells or CD34<sup>+</sup> cells plus MG132 were then added to the fibroblasts and cultured for various time points. MG132 was added 10 minutes before addition of CD34<sup>+</sup> cells. Total RNA was extracted from fibroblast cells after 6 h and 12 h of culture using TRIzol reagent (Invitrogen) following the manufacturer's protocol. Real-time quantitative RT-PCR analysis was performed for MMP-1 and COL1A1 gene expressions. The reverse-transcription was performed using one  $\mu\text{g}$  of mRNA, and the 'High Capacity cDNA Reverse Transcription Kit' (Applied Biosystems, Foster City, CA). One 20<sup>th</sup> of the cDNA was used for the real time PCR analysis. Reactions were performed using SYBR Green PCR master mix (Applied Biosystems) in a Light Cycler 480 (Roche Applied Science) detection system. The primers used were as follows: h-GAPDH, forward 5'-TTTCGACAGTCAGCCGCATCTTCTT, reverse 5'-ACCAAATCCGTTGACTCCGACCTT; h-COL1A1, forward 5'-CAATGCTGCCCTTTCTGCTCCTTT, reverse 5'-CACTTGGGTGTTTGAGCATTGCCT; h-MMP1, forward 5'-ACAGAGATGAAGTCCGGTTT, reverse 5'-GAAGCCAAAGGAGCTGTAGAT. Expression levels of genes were normalized to GAPDH expression level.

### Western blot analysis

Western blot (WB) analysis for proteins isolated from wound tissue of animals with or without CD34<sup>+</sup> therapy was performed by following the standard procedures. Primary antibodies used were for MMP1,  $\alpha$ -SMA (from Santa Cruz, CA), MMP3, MMP9, MMP13, SM22 $\alpha$  (all from Abcam, USA),  $\beta$  actin, and GAPDH (both from Cell Signaling, Beverly, MA). Mouse, rabbit IgG-HRP conjugated (Cell Signaling, Beverly, MA) and goat IgG-HRP conjugated (Santa Cruz, CA) secondary Abs were used and specific bands were detected using enzyme-linked chemiluminescences (Pierce, IL). Densitometric analysis of developed bands was performed by using UN-SCAN-IT (gel 6.1 version) software. Relative density was calculated using respective GAPDH/  $\beta$ -actin bands.



In a separate experiment, fibroblasts were cultured under serum deprived (1% FBS) conditions. Total protein was extracted in lysis buffer containing protease and phosphatase inhibitors from 5 different conditions of fibroblast cultures, such as added MG132 (10  $\mu$ M), CD34<sup>+</sup> cells, CD34<sup>+</sup> cells plus MG132, or MG132 plus SP 600125 (JNK Inhibitor II, 20  $\mu$ M) (from Calbiochem, Darmstadt, Germany), with medium alone serving as a control at both 6 h and 12 h time points. Twenty micrograms of total proteins were tested by WB analysis for levels of c-Jun and GAPDH (all from Cell Signaling, Beverly, MA) following the above-mentioned techniques.

### Total collagen assay

Fibroblasts were cultured in 1% FBS containing DMEM in the presence or absence of CD34<sup>+</sup> cells. Cell culture supernatants were collected after 24 h of co-culture and stored at  $-20^{\circ}$  C for later estimation of total collagen (types I to V). Total collagen was measured colorimetrically using a Sircol Collagen Assay kit (Newtown Abbey, UK) according to the manufacturer's protocol. Total collagen in the wound tissue (day 5 of post-wounding) was also measured colorimetrically using the similar kit and protocols. Briefly, Sircol dye reagent was added to the cell culture supernatants or tissue extracts, stirred for 30 min at room temperature and centrifuged at 12,000 rpm for 10 min. Absorbance of the bound dye was measured at 555 nm wavelength on a spectrophotometer. The amount of collagen protein in samples was adjusted to the total protein estimated by using the BCA Protein Assay kit (Pierce, Rockford, IL, USA). Collagen concentrations were expressed as  $\mu$ g collagen per milligram of total protein.

### Statistical Analysis

All values were expressed as mean  $\pm$  SEM. Student's 't' test was performed for comparison of data of unpaired samples. A probability (p) value  $<0.05$  was considered significant.

## Results

### Isolation and expansion of human cord blood-derived stem cells

CD133<sup>+</sup> cells were isolated from freshly collected human umbilical cord blood using the auto MACS system, and observed more than 95% cells were observed to be CD133<sup>+</sup>. The isolated CD133<sup>+</sup> cells, which also co-express the CD34 molecule were expanded on nanofiber matrices according to the earlier published protocols, and shown to retain stem cell phenotypes and characteristics [18]. After 10 days of expansion on nanofiber coated plates, the purity of the CD34<sup>+</sup> cells was more than 90% as determined by flow cytometry [18].

### CD34<sup>+</sup> cell therapy accelerate wound closure

The therapeutic potential of adult or fetal stem/progenitor cells for the treatment of cutaneous wounds has been noted in various preclinical models [15,17,22]. To determine the therapeutic efficacy of nanofiber expanded CD34<sup>+</sup> cells in wound healing, we tested the ability of the nanofiber-expanded CD34<sup>+</sup> cells to promote wound closure in an excisional cutaneous wound model generated in immunocompromised mice (NOD/SCID). NOD/SCID mice have often been used for transplantation of human cells due to lower graft rejection, and are a well-established animal model for studying therapeutic efficacy for various disease states including cutaneous wounds [23]. Using a cutaneous wound model, herein we show that nanofiber-expanded CD34<sup>+</sup> cell treatment significantly accelerates wound closure as early as day 3 of post-wounding and became more evident on day 7 of post-wounding in most of the animals studied by morphological image analysis (Fig. 1A). Cumulative analysis of wound closure data revealed that CD34<sup>+</sup> cell therapy significantly enhanced the

percentage wound closure in NOD/SCID mice compared to vehicle-treated control (Fig. 1B) at days 3, 5, and 7, indicating a potential use of these cells for cutaneous wound therapy.

### **Nanofiber expanded CD34<sup>+</sup> cells recruited to the wound bed**

To analyze the recruitment of CD34<sup>+</sup> cells to the wound bed, nanofiber expanded CD34<sup>+</sup> cells were transiently transfected with pmaxGFP<sup>+</sup> vector by using the Amaxa electroporation system. More than 90% cells were GFP positive after 24 h and cell viability was more than 70%. GFP positive CD34<sup>+</sup> cells were transplanted within 24 h of transfection. Immunohistochemical analysis of wound tissue sections revealed that a substantial number of GFP<sup>+</sup> cells were present throughout the healing process at days 3, 5 and 7 (Fig. 2A). Quantification of GFP<sup>+</sup> cells showed that 1431±13 GFP<sup>+</sup> cells/mm<sup>2</sup> were present at day 3, while the number of GFP<sup>+</sup> cells decreased at day 5 and day 7 (936±22 GFP<sup>+</sup> cells/mm<sup>2</sup> at day 5; 196±14 GFP<sup>+</sup> cells/mm<sup>2</sup> at day 7) in the wound bed (Fig. 2B). These results indicate that nanofiber-expanded CD34<sup>+</sup> cells were recruited to the wound bed after systemic administration and stayed within the wound bed during the wound healing process.

### **CD34<sup>+</sup> cell therapy enhances fibroblast and myofibroblast levels in the wound bed**

Fibroblast cells are one of the most important cell types in the skin, providing mechanical strength, and producing ECM, which in turn provides mechanical support for the cells within the dermis [3]. Fibroblasts within the dermis differentiate into myofibroblasts, which are responsible for wound contraction. We wanted to investigate whether CD34<sup>+</sup> cell therapy-mediated accelerated healing was due to the increased number of fibroblast/myofibroblasts present in the wound bed. As fibroblasts express SM22 $\alpha$  and myofibroblasts express  $\alpha$ -smooth muscle actin ( $\alpha$ -SMA), we have performed immunohistochemical analysis of the wound edges for those markers at various time points, such as day 5 and 7 after CD34<sup>+</sup> cells therapy or without cell therapy as a control. Immunohistochemical analysis revealed that expression of both  $\alpha$ -SMA and SM22 $\alpha$  markers, indicating fibroblasts and myofibroblasts respectively, were increased in the wounds of animals treated with CD34<sup>+</sup> cells compared to animals that did not receive any cell therapy at day 5 or 7 (Fig. 3A, 3B). Western blot analysis of total protein obtained from the wound tissues supported the conclusion that the mice treated with CD34<sup>+</sup> cells express higher levels of SM22 $\alpha$  compared to vehicle control mice (Fig. 5B). Collectively, these data indicate that higher abundance of fibroblasts and myofibroblasts was evident at the wound bed as a result of CD34<sup>+</sup> cell therapy.

### **CD34<sup>+</sup> cell therapy increases collagen expression in the wound bed**

Collagen present within the ECM is responsible for the strength and resiliency of the skin, and mediates effective healing of the wounds [3,4]. To investigate the amount of collagen present in the wound tissue, sections were subjected to Masson's trichrome staining. Masson's trichrome staining indicated that CD34<sup>+</sup> cell therapy was associated with higher abundance of collagen at the wound bed compared to vehicle treated control at day 5 or 7 (Fig. 4A). To quantify the total amount of collagens present in the tissues, homogenization of the total tissues was performed and supernatants were collected after centrifugation. Total collagen estimation assay (Sircol) was performed using tissue lysates, and it was found that collagen content was elevated in animals which received CD34<sup>+</sup> cell therapy compared to animals which did not receive cells (Fig. 4B). However, the increased collagen content in the wounds of CD34<sup>+</sup> cell treated animals was not significantly different (p=0.06) from control wounds. To study this effect further, immunohistochemical analysis of wound tissues was performed to investigate the presence of procollagen 1A1 (pro-COL1A1), the primary component of collagen 1. Immunohistochemical staining detected higher expression of pro-COL1A1 in the wound sections of animals that received CD34<sup>+</sup> cell therapy

compared to vehicle-treated control (Fig. 4C). This result indicates that CD34<sup>+</sup> cell therapy mediates enhanced collagen deposition at the wound bed during the course of healing.

### **CD34<sup>+</sup> cell therapy reduces levels of matrix metalloproteinases**

MMPs play important role in many stages of wound-healing process, including inflammation, angiogenesis and remodeling [5], while TIMPs are the endogenous inhibitors of MMPs. Therefore, we sought to assess the expression levels of various MMPs and TIMP1 in the wound tissues of animals which had either received CD34<sup>+</sup> cell therapy or vehicle only. WB analysis revealed a significant reduction (Fig. 5A, 5B) in the levels of MMP1, MMP 3, MMP 9 and MMP 13 in wound tissues of the animals treated with CD34<sup>+</sup> cells at days 3, and 7 compared to the wounds of animals treated with vehicle only, except for the level of MMP 9 at day 3, where no significant difference was observed between the two groups of animals (Fig. 5B). However, CD34<sup>+</sup> cell therapy did not increase TIMP1 levels significantly in the wound tissue compared to control wounds at any time points tested. These results suggest that CD34<sup>+</sup> cell therapy decreases MMP levels in the wounds, whereas TIMP1 is largely unaffected.

### **CD34<sup>+</sup> cells promote fibroblast cell migration and fibroblast cell number *in vitro***

To examine whether CD34<sup>+</sup> cell therapy influences the biological effects of dermal fibroblasts, such as cell migration, we mimicked the cutaneous wound condition *in vitro* using a scratch wound to assess the effect of CD34<sup>+</sup> cells on human dermal fibroblast cells. The scratch wound assay showed that the migration of dermal fibroblasts into the wound area was significantly higher (106±8 cells) in the presence of CD34<sup>+</sup> cells compared to the number of fibroblasts (68±6 cells) in the absence of CD34<sup>+</sup> cells (Fig. 6A, 6B). This result suggests that the presence of CD34<sup>+</sup> cells largely influence the migration of fibroblast cells. The proliferation of fibroblasts is an important aspect of wound healing; therefore we investigated the effects of CD34<sup>+</sup> cells on the expansion of human fibroblast cells *in vitro*. The number of human dermal fibroblasts was significantly enhanced in the presence of CD34<sup>+</sup> cells after 48 h co-culture compared to the fibroblasts without CD34<sup>+</sup> cells (Fig. 6C), indicating that the presence of CD34<sup>+</sup> cells may promote an increase in the numbers of human dermal fibroblasts.

### **CD34<sup>+</sup> cells synthesize/secrete collagen**

To determine whether the CD34<sup>+</sup> cells synthesize/secrete collagens to contribute to the accelerated wound healing process, we tested total collagen synthesis/secretion in the cell culture supernatants at various time points using a Sircol collagen assay kit without any added stimulus except serum deprivation. The total collagen assay revealed that CD34<sup>+</sup> cells synthesize/secrete collagen under serum-deprived conditions, and that the amount of collagen is significantly higher at 24 h or 48 h time points compared to the basal condition (0 h time point) (Fig. 7). These results confirm that CD34<sup>+</sup> cells not only mediate enhanced synthesis of collagen *in vivo*, but also synthesize/secrete collagen by themselves to facilitate the wound-healing process.

### **CD34<sup>+</sup> cells influence expression of MMP1 and COL1A1 in dermal fibroblast cells**

As dermal fibroblasts play a critical role in ECM formation [3], we investigated the mechanism by which CD34<sup>+</sup> cells regulate the functionality of dermal fibroblast cells. Among the MMPs, MMP1 plays a predominant role in degrading dermal type I collagen [8,24]. COL1A1 is the primary component of type I collagen, a major component of ECM in the skin [24]. A delicate balance between collagen synthesis and MMP activity is important for ECM turnover. Thus, we sought to further explore the effect of CD34<sup>+</sup> cells on the expression of MMP1 and COL1A1 in dermal fibroblast cells using the quantitative RT-PCR



method. Real time RT-PCR analysis revealed that COL1A1 synthesis in dermal fibroblasts was significantly enhanced after co-culture with CD34<sup>+</sup> cells at various time points studied compared to the fibroblasts cultured alone (Fig. 8A, upper panel, left). On the other hand, MMP1 synthesis in dermal fibroblasts was significantly reduced after coculture with CD34<sup>+</sup> cells compared to the fibroblasts cultured alone. These results indicate that CD34<sup>+</sup> cells influence the fibrogenic activity of dermal fibroblast cells (Fig. 8A, lower panel, left).

To confirm the specificity of CD34<sup>+</sup> cells in regulating the expression of MMP1 and COL1A1 in dermal fibroblast cells, we assessed levels of MMP1 and COL1A1 in the presence of a proteasome inhibitor (MG132), a known inhibitor of COL1A1, and a stimulator of MMP1 expression, using RT-PCR methods [25]. Quantitative RT-PCR analysis revealed that MG132 significantly reduced expression of COL1A1 in dermal fibroblasts, whereas COL1A1 expression was restored or partially restored by CD34<sup>+</sup> cells at 3 h or 6 h respectively under the same experimental conditions (Fig. 8A, upper panel, right). On the other hand, MG132 significantly increased the expression of MMP1 in dermal fibroblasts at all of the time points tested. On the other hand, CD34<sup>+</sup> cells at 12 h significantly decreased MMP1 expression under similar experimental conditions (Fig. 8A, lower panel, right). This result indicates that CD34<sup>+</sup> cells influence the expression of both MMP1 and COL1A1 in fibroblast cells.

### **CD34<sup>+</sup> cells suppress proteasome inhibitor-mediated c-Jun levels in dermal fibroblasts**

To specifically define the molecular pathway involved in this process, we chose to examine the JNK pathway, as it is known that MG132 specifically induces an increase in c-Jun level, which primarily regulates decreased COL1A1 and increased MMP1 synthesis [25]. Therefore, we investigated whether CD34<sup>+</sup> cells have any effect on levels of c-Jun molecule in dermal fibroblasts in the presence or absence of MG132. WB analysis revealed that c-Jun expression in fibroblast cells was increased in the presence of MG132, whereas in the presence of both CD34<sup>+</sup> cells and MG132, the level of c-Jun was decreased significantly at various time points tested (Fig. 8B). A JNK inhibitor also reduced the level of c-Jun in the presence of MG132, confirming the involvement of the JNK pathway (Fig. 8B).

## **Discussion**

Although significant advancement has been made in all aspects of wound healing therapy, still a large number of amputations occur each year due to the refractory wounds, which impose a burden on the economy and patient's lives [26]. Cell-based therapies show promise in healing wounds in various models, however mechanistic pathways have not yet been investigated in detail other than angiogenesis [15,22]. A limitation in procurement of an adequate number of stem cells has long hindered the success of cellbased therapeutic intervention for degenerative diseases. However, our established CD34<sup>+</sup> cell expansion method provides an adequate number of stem cells for preclinical evaluations in various ischemic and degenerative disease models [18,19,27]. However, their potential for treating wounds and their underlying mechanisms of action are previously unexplored. Recently identified telocytes, resemble with "dendritic cells", which are also positive for CD34 marker, present in the human dermis, might play role in skin regeneration [28]. However, morphologically telocytes are significantly different from nanofiber expanded cord blood derived CD34<sup>+</sup> cells, which remain round in shape after nanofiber expansion. The human umbilical cord blood-derived stem cell, as a unit, has been the basis for an important regimen for treating multiple hematological disorders for more than five decades [29,30]. Additionally, human cord blood-derived stem cells are currently being used for regenerative studies as they possess minimal oncogenic transformation capabilities, and display stable telomeres, which also serve to protect against potential oncogenic transformation [31–33]. Moreover, we have not observed oncogenic transformation of transplanted CD34<sup>+</sup> cells in

various preclinical models in our previous studies [18,19,27,34]. Using peripheral blood-derived CD34<sup>+</sup> cells in a wound healing model, another laboratory also did not show any oncogenic transformation of CD34<sup>+</sup> cells [22], suggesting that CD34<sup>+</sup> cell transplantation is safe. In our current study, nanofiber-expanded human umbilical cord blood-derived CD34<sup>+</sup> cell therapy improved wound healing and accelerated cutaneous wound closure in NOD/SCID mice (Fig. 1A, 1B), consistent with the previous observations of blood derived stem cell mediated accelerated wound healing [15,22]. This accelerated wound closure was mediated by efficient recruitment of nanofiber expanded CD34<sup>+</sup> cells to the wound bed, as a substantial number of GFP<sup>+</sup> CD34<sup>+</sup> cells were observed at the wound bed after tail vein administration (Fig. 2A, 2B). The recruitment of CD34<sup>+</sup> cells to the wound bed was facilitated by the constitutive expression of CXCR4 on the surface of CD34<sup>+</sup> cells after nanofiber expansion [18], which correlated well with previous observations where expression of CXCR4 on the surface of hematopoietic stem cells helps their preferential migration to the inflammatory or ischemic areas [35,36].

An open wound injury requires the well-orchestrated integration of complex biological and molecular events for its healing [1,2]. It is well known that both fibroblasts and myofibroblasts play critical roles in the wound healing process. Specifically, the traction forces of fibroblasts and coordinated contraction of myofibroblasts facilitate accelerated wound contraction and closure [37]. In our present study, we observed that animals, treated with CD34<sup>+</sup> cells, in comparison to control, have higher abundance of myofibroblasts, expressing  $\alpha$ -SMA [12], at the wound bed (Fig. 3). This observation correlated well with accelerated wound closure in CD34<sup>+</sup> cell-treated animals (Fig. 1). Myofibroblasts in cutaneous wounds are generally believed to evolve from resident fibroblasts in the dermis and subcutaneous tissues surrounding the wound [38]. Along with other cells, fibroblast cells express the SM22 $\alpha$  protein [39]. We have found a higher abundance of SM22 $\alpha$  positive cells at the wound bed of CD34<sup>+</sup> cell-treated animals (Fig. 3, 5B), indicating a higher number of fibroblast cells at the dermis area of wounds, which probably later on differentiate into myofibroblasts, as indicated by higher expression of  $\alpha$ -SMA positive cells. However, in pathological conditions such as diabetes, fibroblasts fail to respond to injury due to impaired proliferation capabilities [40]. Hence, improving functionality in fibroblast migration and proliferation could be a strategy to achieve normal wound healing. In this study, we have further demonstrated *in vitro* that CD34<sup>+</sup> cells could enhance migration and most likely proliferation of dermal fibroblasts at the wound area (Fig. 6A, 6B, 6C). However, this will be tested more conclusively in future studies where the use of proliferation markers will clearly demonstrate the capability of CD34<sup>+</sup> cells to mediated fibroblast proliferation.

Fibroblasts and myofibroblasts also play pivotal roles in the continuous deposition of ECM proteins, such as collagen types I to VI, which are essential components for wound healing [12,41]. Interestingly, we found a higher intensity of collagen staining in the wounds of animals treated with CD34<sup>+</sup> cells compared to those without CD34<sup>+</sup> cells (Fig. 4A), indicating a role of CD34<sup>+</sup> cells in promoting collagen formation. After quantifying, the total amount of collagen present in the wound tissues, we found that the collagen content was much higher in the wounds of animals treated with CD34<sup>+</sup> cells compared to the controls, but not statistically significant (Fig. 4B). To identify the sources of collagens, we conducted a test *in vitro* and found that CD34<sup>+</sup> cells themselves secrete a significant amount of collagen (Fig. 7). Type-I collagen is a major component of ECM in the skin. We also observed a higher abundance of procollagen1a in the wounds of animals treated with CD34<sup>+</sup> cells compared to the controls (Fig. 4C). This *in vivo* observation was confirmed *in vitro* when human fibroblasts were co-cultured with CD34<sup>+</sup> cells, after which COL1A1 expression was significantly increased compared to fibroblasts alone (Fig. 8A). In addition, in the presence of the specific proteasome inhibitor MG132, the expression of COL1A1 was

decreased, which was consistent with earlier studies [25]. However, the expression of COL1A1 by dermal fibroblasts in presence of MG132 was recovered with the co-culture of CD34<sup>+</sup> cells (Fig. 8A), indicating a positive regulation of collagen synthesis and ECM formation by CD34<sup>+</sup> cells during the wound healing process.

MMPs are primarily involved in the remodeling of ECM. However, uncontrolled activity of MMPs is often associated with delayed, deficient or impaired wound closure [42]. Reports show that the expression levels of MMPs are markedly elevated in chronic ulcers compared to normal wounds [6,43,44], as these proteinases degrade essential ECM components, integrin receptors, growth factors, and their receptors, which are essential components for healing [45]. In our present study, CD34<sup>+</sup> cell therapy resulted in decreased levels of MMP-1, -3, -9, and -13 in wounds (Fig. 5), and was highly associated with faster wound healing, due at least in part to the limited degradation of critical ECM components and other essential factors. Activity of these MMPs is known to depend on binding to endogenous inhibitors such as tissue inhibitor of metalloproteinases (TIMP) [11], and higher TIMP expression, thus, may contribute to higher ECM turnover. We observed higher expression of TIMP1 in some CD34<sup>+</sup> cell treated wound tissues, but did not find a significant difference from control wounds (Fig. 5A, 5B). Hence, the impact of CD34<sup>+</sup> cell therapy on the regulation of TIMP1 is inconclusive. Furthermore, MMP-1 in particular has a distinct role in cleaving the triple helix of type I collagen, allowing the chains to unwind and become susceptible to further degradation [8]. Not only does CD34<sup>+</sup> cell therapy have the ability to down regulate MMP1 protein at the wound tissue (Fig.5A, 5B), but these CD34<sup>+</sup> stem cells also have the ability to suppress the expression of MMP1 in dermal fibroblasts *in vitro* (Fig. 8A), even in the presence of a proteasome inhibitor (8A), known to increase the synthesis of MMP1 in dermal fibroblasts [25].

In summary, CD34<sup>+</sup> cell therapy accelerates wound healing by enhancing collagen synthesis and reducing MMP production in the wound bed via migration of fibroblasts into the wound bed. Although the potential clinical application of CD34<sup>+</sup> cells remains to be investigated, this study serves as a proof of concept that CD34<sup>+</sup> cell therapy could be considered a useful strategy for the treatment of refractory wounds where wound contraction, extracellular matrix deposition and tissue remodeling is severely compromised.

## Acknowledgments

This work was part of the PhD dissertation thesis of Suman Kanji. This work was supported in part by National Institutes of Health grants, K01 AR054114 (NIAMS), SBIR R44 HL092706-01 (NHLBI), Pelotonia IDEA Award, and The Ohio State University start-up fund. Nanofiber-coated plates were kind gift from Hai-Quan Mao (John's Hopkins University, MD). Human primary skin fibroblast cells were kind gift from Heather M. Powell, The Ohio State University.

## References

1. Singer AJ, Clark RA. Cutaneous wound healing. *N Engl J Med.* 1999; 341:738–746. [PubMed: 10471461]
2. Martin P. Wound healing--aiming for perfect skin regeneration. *Science.* 1997; 276:75–81. [PubMed: 9082989]
3. Le Pillouer-Prost A. Fibroblasts: what's new in cellular biology? *J Cosmet Laser Ther.* 2003; 5:232–238. [PubMed: 14741842]
4. Gosain A, DiPietro LA. Aging and wound healing. *World J Surg.* 2004; 28:321–326. [PubMed: 14961191]
5. Soo C, Shaw WW, Zhang X, et al. Differential expression of matrix metalloproteinases and their tissue-derived inhibitors in cutaneous wound repair. *Plast Reconstr Surg.* 2000; 105:638–647. [PubMed: 10697171]

6. Weckroth M, Vaheri A, Lauharanta J, et al. Matrix metalloproteinases, gelatinase and collagenase, in chronic leg ulcers. *J Invest Dermatol.* 1996; 106:1119–1124. [PubMed: 8618050]
7. Nagase H, Woessner JF Jr. Matrix metalloproteinases. *J Biol Chem.* 1999; 274:21491–21494. [PubMed: 10419448]
8. Shapiro SD. Matrix metalloproteinase degradation of extracellular matrix: biological consequences. *Curr Opin Cell Biol.* 1998; 10:602–608. [PubMed: 9818170]
9. Vaalamo M, Mattila L, Johansson N, et al. Distinct populations of stromal cells express collagenase-3 (MMP-13) and collagenase-1 (MMP-1) in chronic ulcers but not in normally healing wounds. *J Invest Dermatol.* 1997; 109:96–101. [PubMed: 9204962]
10. Xue M, Le NT, Jackson CJ. Targeting matrix metalloproteases to improve cutaneous wound healing. *Expert Opin Ther Targets.* 2006; 10:143–155. [PubMed: 16441234]
11. Vincenti MP. The matrix metalloproteinase (MMP) and tissue inhibitor of metalloproteinase (TIMP) genes. Transcriptional and posttranscriptional regulation, signal transduction and cell-type-specific expression. *Methods Mol Biol.* 2001; 151:121–148. [PubMed: 11217296]
12. Powell DW, Mifflin RC, Valentich JD, et al. Myofibroblasts. I. \*\*Paracrine cells important in health and disease. *Am J Physiol.* 1999; 277:C1–C9. [PubMed: 10409103]
13. Karsenty G, de Crombrugge B. Conservation of binding sites for regulatory factors in the coordinately expressed alpha 1 (I) and alpha 2 (I) collagen promoters. *Biochem Biophys Res Commun.* 1991; 177:538–544. [PubMed: 2043139]
14. Sen CK, Gordillo GM, Roy S, et al. Human skin wounds: a major and snowballing threat to public health and the economy. *Wound Repair Regen.* 2009; 17:763–771. [PubMed: 19903300]
15. Barcelos LS, Duplaa C, Krinkel N, et al. Human CD133+ progenitor cells promote the healing of diabetic ischemic ulcers by paracrine stimulation of angiogenesis and activation of Wnt signaling. *Circ Res.* 2009; 104:1095–1102. [PubMed: 19342601]
16. Suh W, Kim KL, Kim JM, et al. Transplantation of endothelial progenitor cells accelerates dermal wound healing with increased recruitment of monocytes/macrophages and neovascularization. *Stem Cells.* 2005; 23:1571–1578. [PubMed: 16081667]
17. Kim JY, Song SH, Kim KL, et al. Human cord blood-derived endothelial progenitor cells and their conditioned media exhibit therapeutic equivalence for diabetic wound healing. *Cell Transplant.* 2010; 19:1635–1644. [PubMed: 20659357]
18. Das H, Abdulhameed N, Joseph M, et al. Ex vivo nanofiber expansion and genetic modification of human cord blood-derived progenitor/stem cells enhances vasculogenesis. *Cell Transplant.* 2009; 18:305–318. [PubMed: 19558779]
19. Das H, George JC, Joseph M, et al. Stem cell therapy with overexpressed VEGF and PDGF genes improves cardiac function in a rat infarct model. *PLoS One.* 2009; 4:e7325. [PubMed: 19809493]
20. Marrotte EJ, Chen DD, Hakim JS, et al. Manganese superoxide dismutase expression in endothelial progenitor cells accelerates wound healing in diabetic mice. *J Clin Invest.* 2010; 120:4207–4219. [PubMed: 21060152]
21. Liang CC, Park AY, Guan JL. In vitro scratch assay: a convenient and inexpensive method for analysis of cell migration in vitro. *Nat Protoc.* 2007; 2:329–333. [PubMed: 17406593]
22. Sivan-Loukianova E, Awad OA, Stepanovic V, et al. CD34+ blood cells accelerate vascularization and healing of diabetic mouse skin wounds. *J Vasc Res.* 2003; 40:368–377. [PubMed: 12891006]
23. Grunewald M, Avraham I, Dor Y, et al. VEGF-induced adult neovascularization: recruitment, retention, and role of accessory cells. *Cell.* 2006; 124:175–189. [PubMed: 16413490]
24. Ghosh AK. Factors involved in the regulation of type I collagen gene expression: implication in fibrosis. *Exp Biol Med (Maywood).* 2002; 227:301–314. [PubMed: 11976400]
25. Fineschi S, Reith W, Guerne PA, et al. Proteasome blockade exerts an antifibrotic activity by coordinately down-regulating type I collagen and tissue inhibitor of metalloproteinase-1 and up-regulating metalloproteinase-1 production in human dermal fibroblasts. *Faseb J.* 2006; 20:562–564. [PubMed: 16410344]
26. Brem H, Sheehan P, Rosenberg HJ, et al. Evidence-based protocol for diabetic foot ulcers. *Plast Reconstr Surg.* 2006; 117:193S–209S. discussion 10S–11S. [PubMed: 16799388]

27. Aggarwal R, Lu J, Kanji S, et al. Human umbilical cord blood-derived CD34+ cells reverse osteoporosis in NOD/SCID mice by altering osteoblastic and osteoclastic activities. *PLoS One*. 2012; 7:e39365. [PubMed: 22724005]
28. Ceafalan L, Gherghiceanu M, Popescu LM, et al. Telocytes in human skin--are they involved in skin regeneration? *J Cell Mol Med*. 2012; 16:1405–1420. [PubMed: 22500885]
29. Ljungman P, Bregni M, Brune M, et al. Allogeneic and autologous transplantation for haematological diseases, solid tumours and immune disorders: current practice in Europe 2009. *Bone Marrow Transplant*. 2009; 45:219–234. [PubMed: 19584824]
30. Mimeault M, Batra SK. Concise review: recent advances on the significance of stem cells in tissue regeneration and cancer therapies. *Stem Cells*. 2006; 24:2319–2345. [PubMed: 16794264]
31. Fiorina P, Voltarelli J, Zavazava N. Immunological applications of stem cells in type 1 diabetes. *Endocr Rev*. 2011; 32:725–754. [PubMed: 21862682]
32. McGuckin CP, Forraz N. Potential for access to embryonic-like cells from human umbilical cord blood. *Cell Prolif*. 2008; 41(Suppl 1):31–40. [PubMed: 18181943]
33. Oh W, Kim DS, Yang YS, et al. Immunological properties of umbilical cord blood-derived mesenchymal stromal cells. *Cell Immunol*. 2008; 251:116–123. [PubMed: 18495100]
34. Lu J, Kanji S, Aggarwal R, et al. Hematopoietic stem cells improve dopaminergic neuron in the MPTP-mice. *Front Biosci*. 2013; 18:970–981.
35. Aiuti A, Webb IJ, Bleul C, et al. The chemokine SDF-1 is a chemoattractant for human CD34+ hematopoietic progenitor cells and provides a new mechanism to explain the mobilization of CD34+ progenitors to peripheral blood. *J Exp Med*. 1997; 185:111–120. [PubMed: 8996247]
36. Jo DY, Rafii S, Hamada T, et al. Chemotaxis of primitive hematopoietic cells in response to stromal cell-derived factor-1. *J Clin Invest*. 2000; 105:101–111. [PubMed: 10619866]
37. Tomasek JJ, Gabbiani G, Hinz B, et al. Myofibroblasts and mechano-regulation of connective tissue remodelling. *Nat Rev Mol Cell Biol*. 2002; 3:349–363. [PubMed: 11988769]
38. Ross R, Everett NB, Tyler R. Wound healing and collagen formation. VI. The origin of the wound fibroblast studied in parabiosis. *J Cell Biol*. 1970; 44:645–654. [PubMed: 5415241]
39. Yamamura H, Masuda H, Ikeda W, et al. Structure and expression of the human SM22alpha gene, assignment of the gene to chromosome 11, and repression of the promoter activity by cytosine DNA methylation. *J Biochem*. 1997; 122:157–167. [PubMed: 9276683]
40. Loots MA, Lamme EN, Mekkes JR, et al. Cultured fibroblasts from chronic diabetic wounds on the lower extremity (non-insulin-dependent diabetes mellitus) show disturbed proliferation. *Arch Dermatol Res*. 1999; 291:93–99. [PubMed: 10195396]
41. Eckes B, Kessler D, Aumailley M, et al. Interactions of fibroblasts with the extracellular matrix: implications for the understanding of fibrosis. *Springer Semin Immunopathol*. 1999; 21:415–429. [PubMed: 10945034]
42. Menke NB, Ward KR, Witten TM, et al. Impaired wound healing. *Clin Dermatol*. 2007; 25:19–25. [PubMed: 17276197]
43. Ladwig GP, Robson MC, Liu R, et al. Ratios of activated matrix metalloproteinase-9 to tissue inhibitor of matrix metalloproteinase-1 in wound fluids are inversely correlated with healing of pressure ulcers. *Wound Repair Regen*. 2002; 10:26–37. [PubMed: 11983004]
44. Trengove NJ, Stacey MC, MacAuley S, et al. Analysis of the acute and chronic wound environments: the role of proteases and their inhibitors. *Wound Repair Regen*. 1999; 7:442–452. [PubMed: 10633003]
45. Mast BA, Schultz GS. Interactions of cytokines, growth factors, and proteases in acute and chronic wounds. *Wound Repair Regen*. 1996; 4:411–420. [PubMed: 17309691]



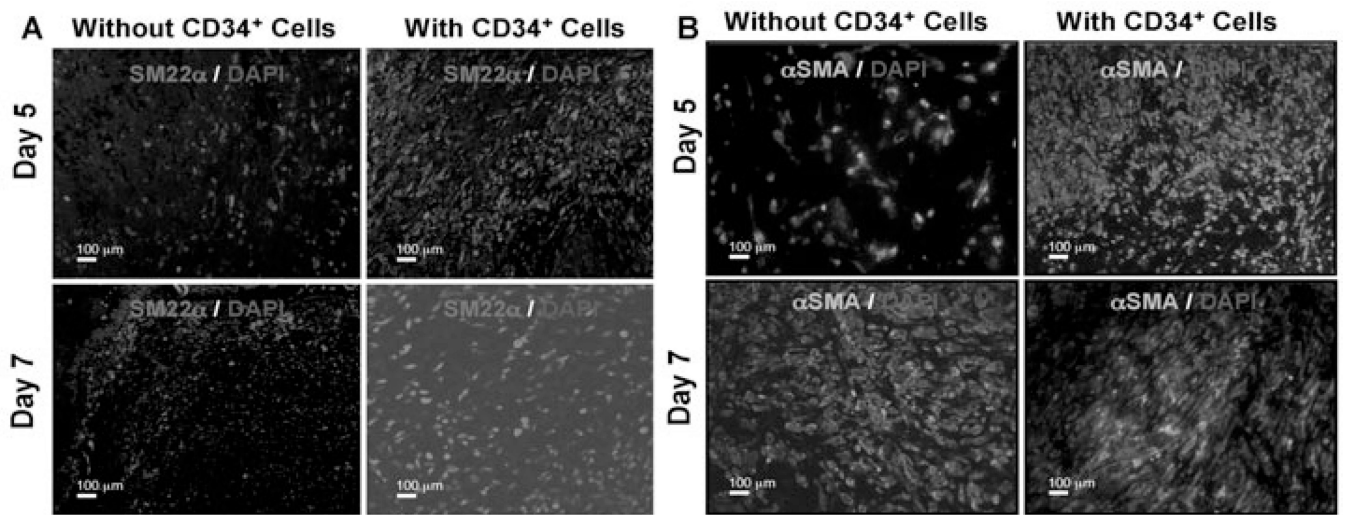


**Figure 1. Nanofiber-expanded CD34<sup>+</sup> cell therapy accelerates wound closure in NOD/SCID mice**  
**A.** Morphological images of cutaneous wounds (8 mm punch biopsies) in NOD/SCID mice at day 0, 3, 5, and 7 of post wounding with or without CD34<sup>+</sup> cell therapy. **B.** Graphical presentation of cumulative measurement of percent wound closure on day 0, 3, 5, and 7 with or without CD34<sup>+</sup> cell therapy. Results are shown as mean  $\pm$  SEM (on day 3, n=12; day 5, n=9; day 7, n=6).

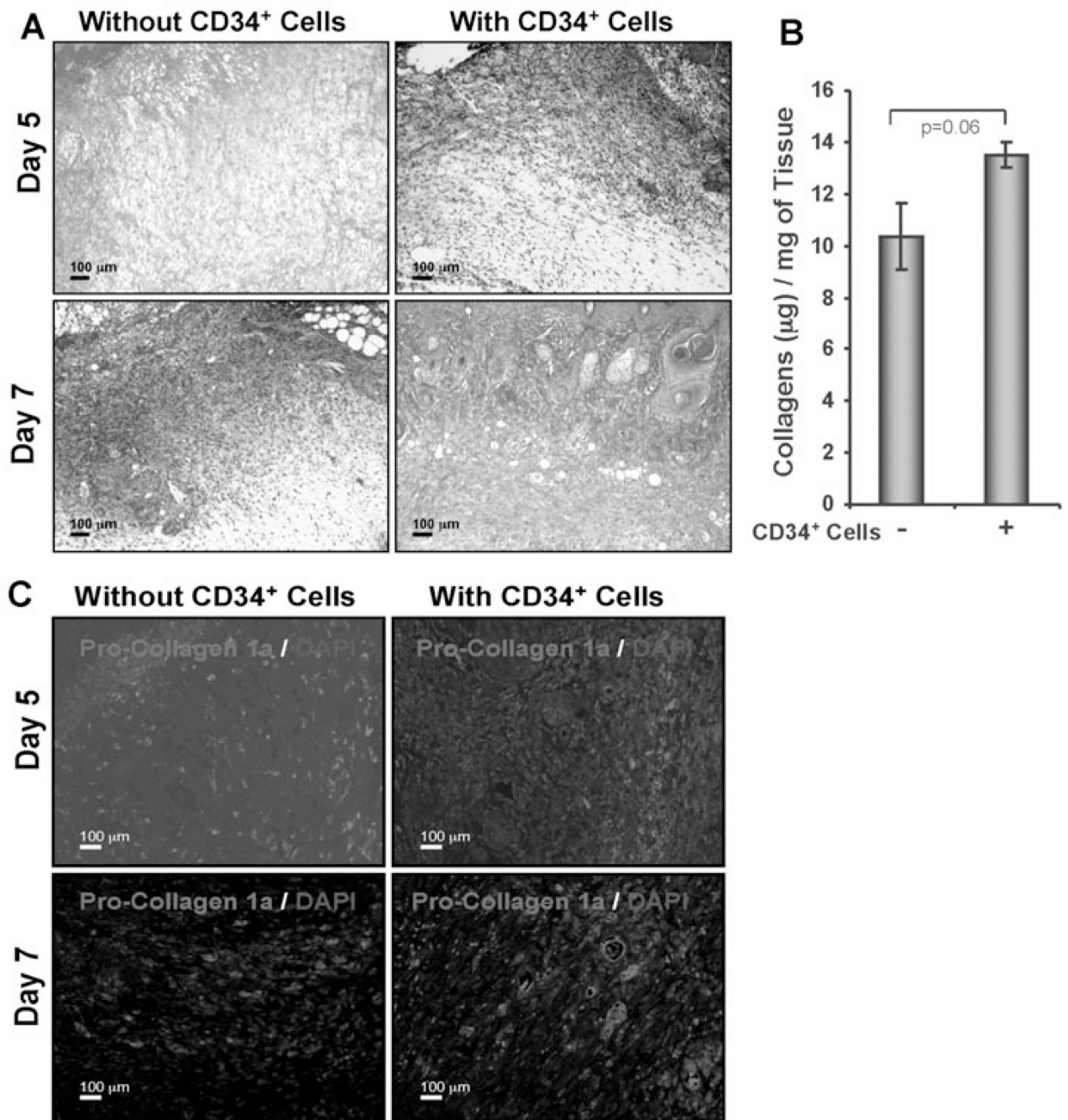


**Figure 2. Nanofiber-expanded CD34<sup>+</sup> cells were recruited to the wound bed**  
**A.** Green fluorescence protein (GFP) was overexpressed on nanofiber-expanded CD34<sup>+</sup> cells using Amaxa nucleoporation system, were assessed for homing to the wound bed at various time points by using  $\alpha$ -GFP Ab by immunohistochemical methods. **B.** Quantitative values of GFP<sup>+</sup> cells were presented graphically. GFP<sup>+</sup> cells were quantified by counting the cells in randomly chosen 8 high power microscopic fields within the wound edge sections (n=3) obtained from various time points (day 3, 5, and 7). Data are presented as mean  $\pm$  SEM.

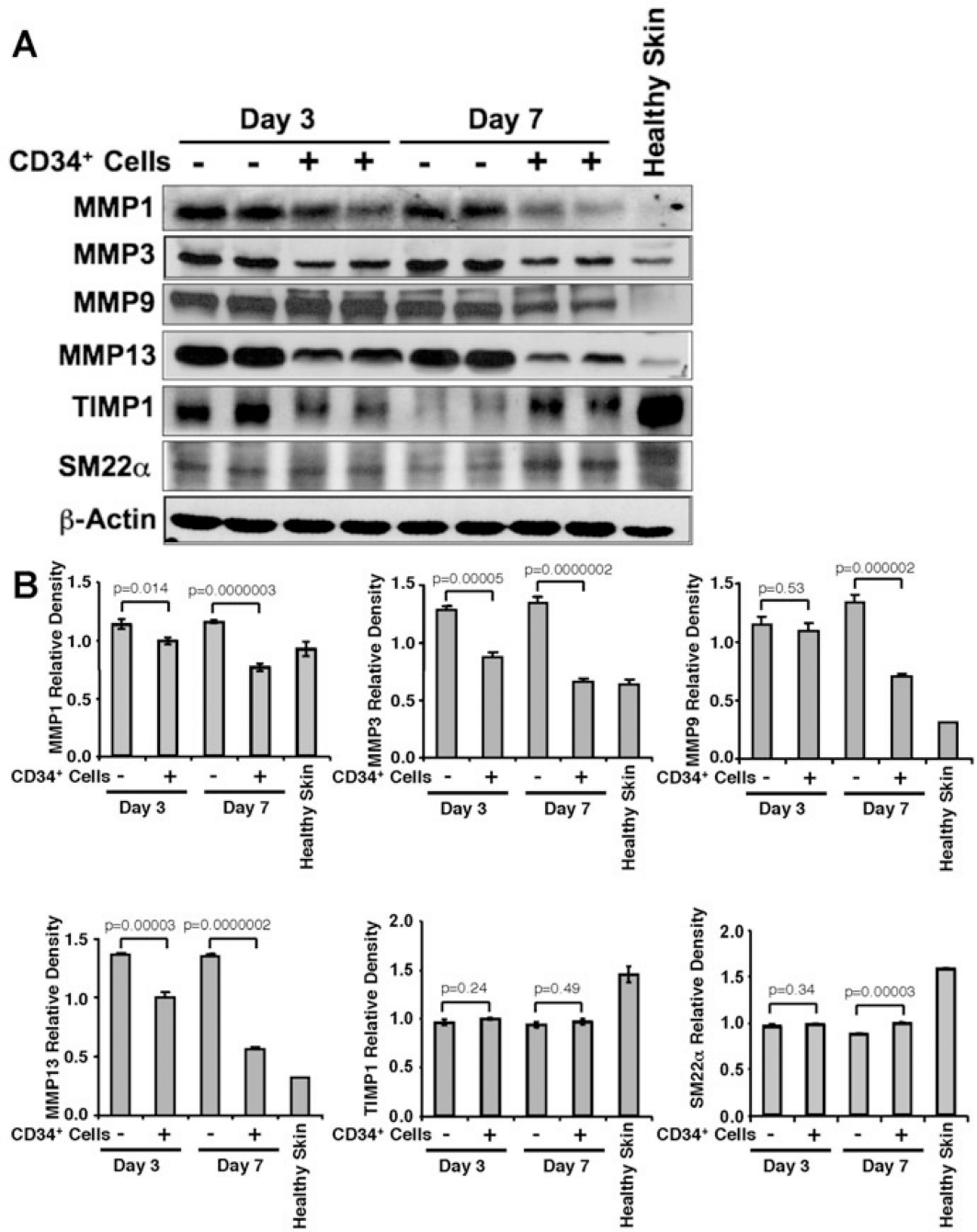


**Figure 3. Enhanced fibroblast and myofibroblast cells in response to CD34<sup>+</sup> cell therapy**  
 Immunofluorescence mediated detection of (A) fibroblast (SM22- $\alpha$ ), and (B) myofibroblast (alpha smooth muscle actin,  $\alpha$ -SMA) cells in the wound bed of animals received CD34<sup>+</sup> cells or without cells as a control at various time points of therapy.

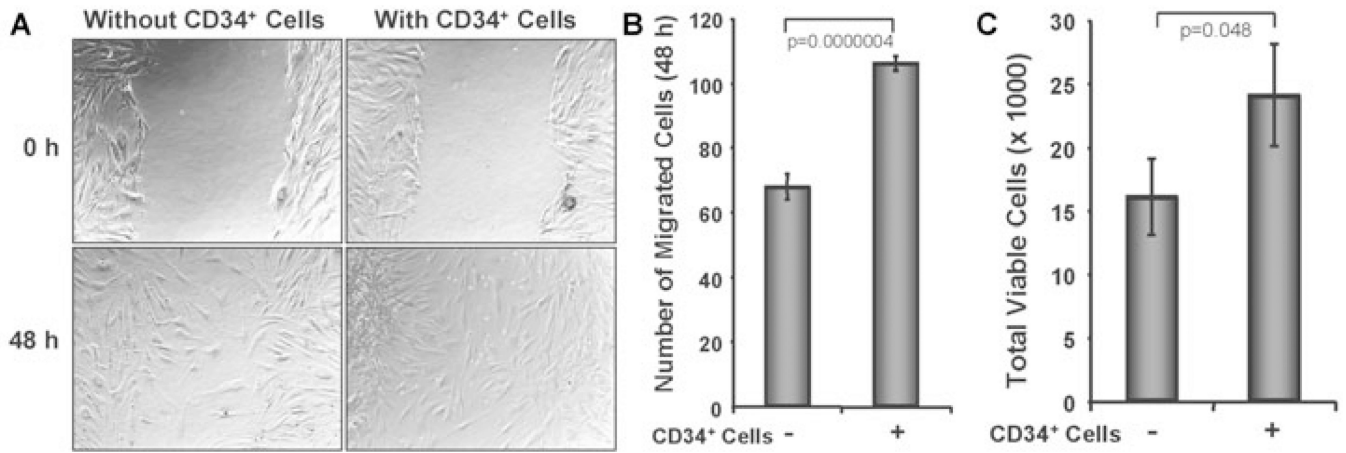


**Figure 4. Enhanced collagen deposition in response to CD34<sup>+</sup> cell therapy**

**A.** Masson's Trichrome staining (blue stain) was performed to the sections of wound edges at various time points. **B.** Graphical presentation of the amount of total collagen in wound skin lysates from the animals (n = 3) received CD34<sup>+</sup> cells or media on day 5 after wounding, measured by using a Sircol Collagen Assay kit. **C.** Immunofluorescence detection of pro-collagen 1A1 (pro-COL1A1) in formalin-fixed paraffin sections of wound edges.

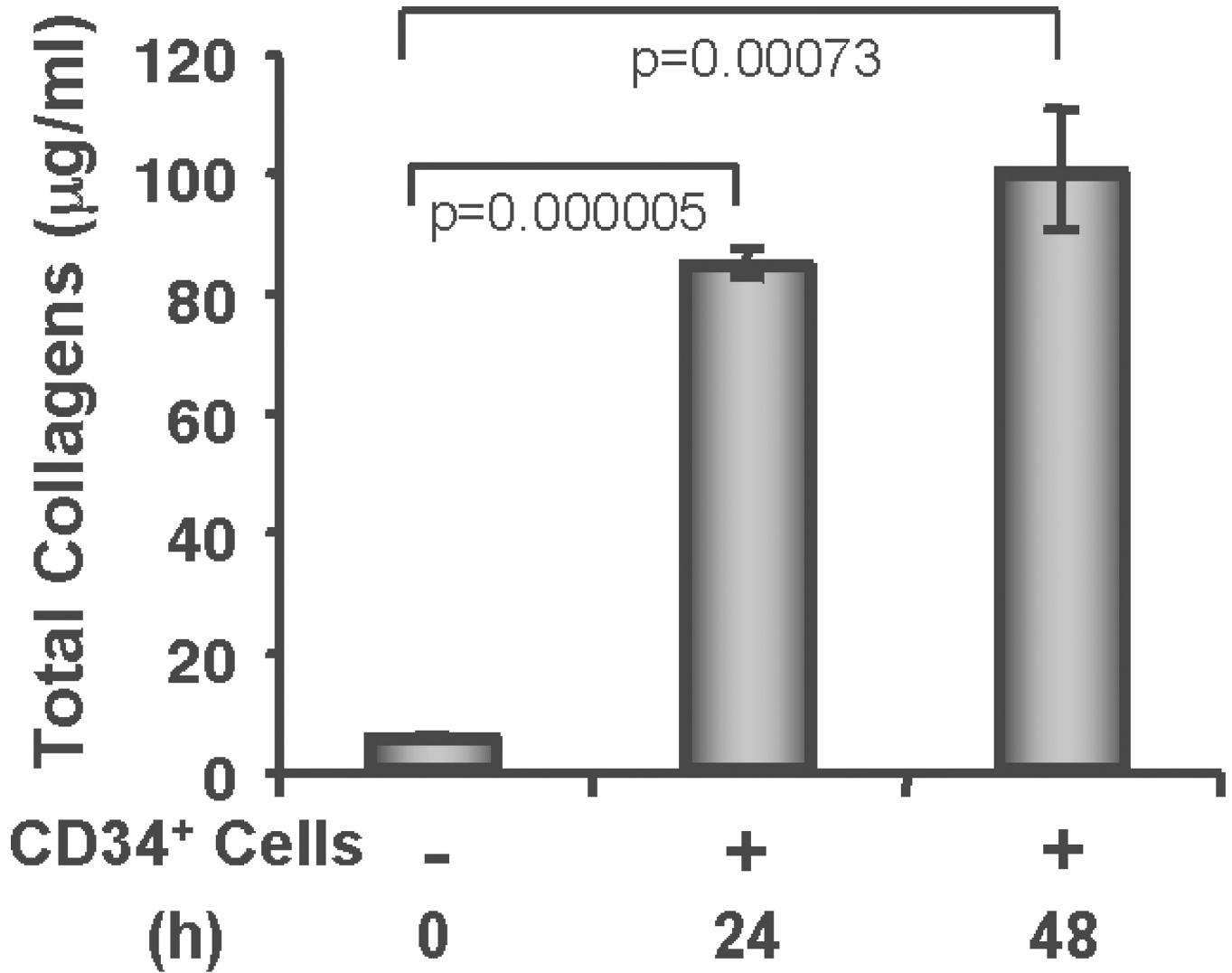


**Figure 5. CD34<sup>+</sup> cell therapy decreased MMP levels in wound tissues**

**A.** Representative western blot analysis of MMP-1, 3, 9, 13, TIMP1, and SM22 $\alpha$  protein levels in wound tissue lysates from mice received CD34<sup>+</sup> cells or media as a control at day 3 and 7 after wounding.  $\beta$ -actin level was used as house keeping protein for loading. **B.**

Quantitative values of each molecule were calculated by performing densitometric analysis of the targeted protein bands and graphically presented relative to  $\beta$ -actin amount. Results are shown as mean  $\pm$  SEM (n=3) within a representative of three independent experiments.



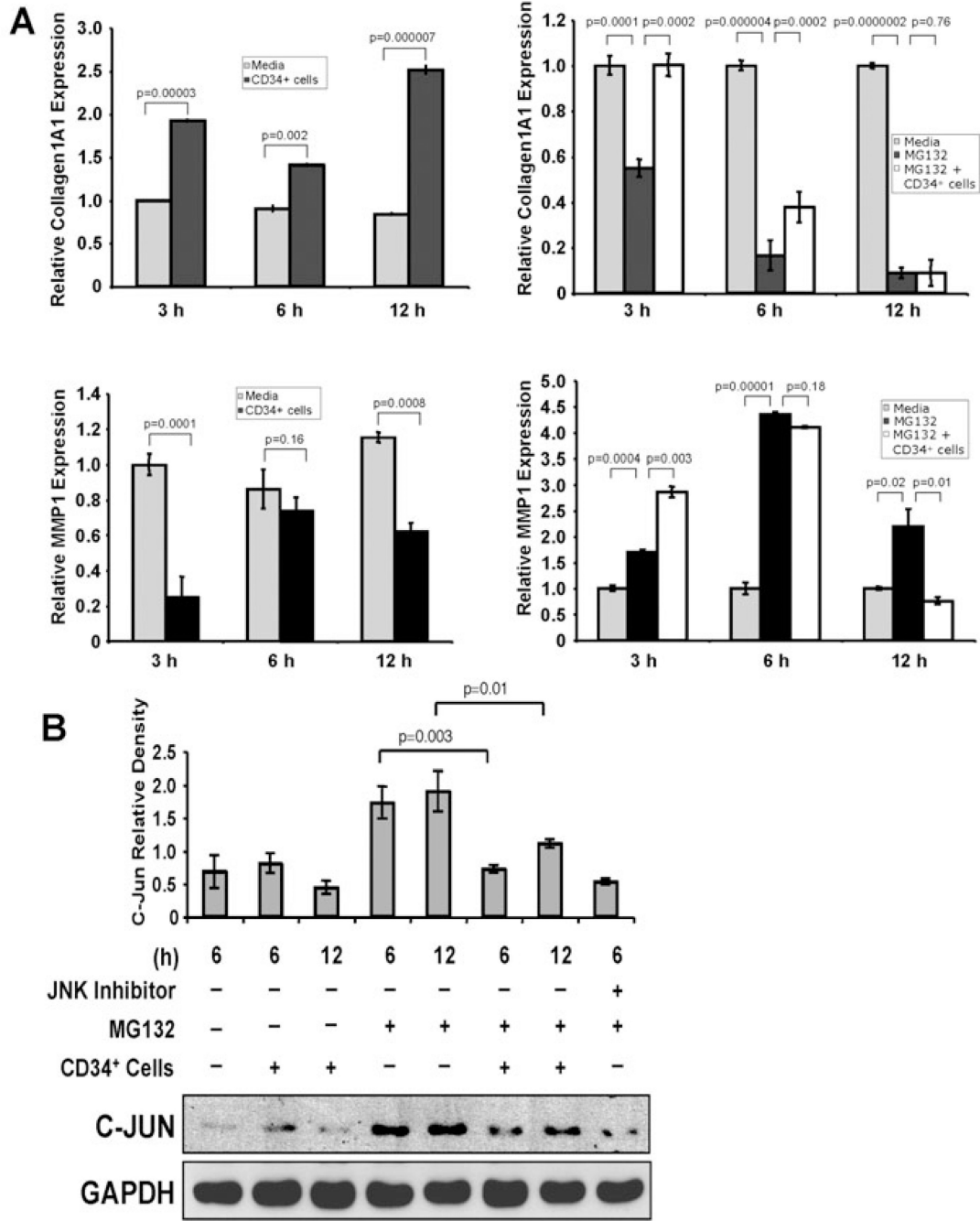


**Figure 6. CD34<sup>+</sup> cells enhance dermal fibroblast cell number and migration**

**A.** Cell migration assay was performed in two-chambered 24-well plate. Confluent dermal fibroblast was grown in lower chamber and monolayer was scratched with a p200 pipette tip. CD34<sup>+</sup> cell containing inserts or without cell inserts (as a control) were placed on the top of well with scratched fibroblast cells. Images for each well were captured immediately after scratch and after 48 h of scratching. **B.** Number of migrated fibroblast cells were counted in presence or absence of CD34<sup>+</sup> cells and presented graphically. **C.** Number of fibroblast cells was counted from the bottom chamber of trans well (24-well) plate after 48 h of co-cultured with CD34<sup>+</sup> cells or media. Non-adherent cells were removed by washing from the lower

chamber before harvesting fibroblasts for analysis. Results are shown as mean  $\pm$  SEM (n=6) within a representative of three independent experiments.

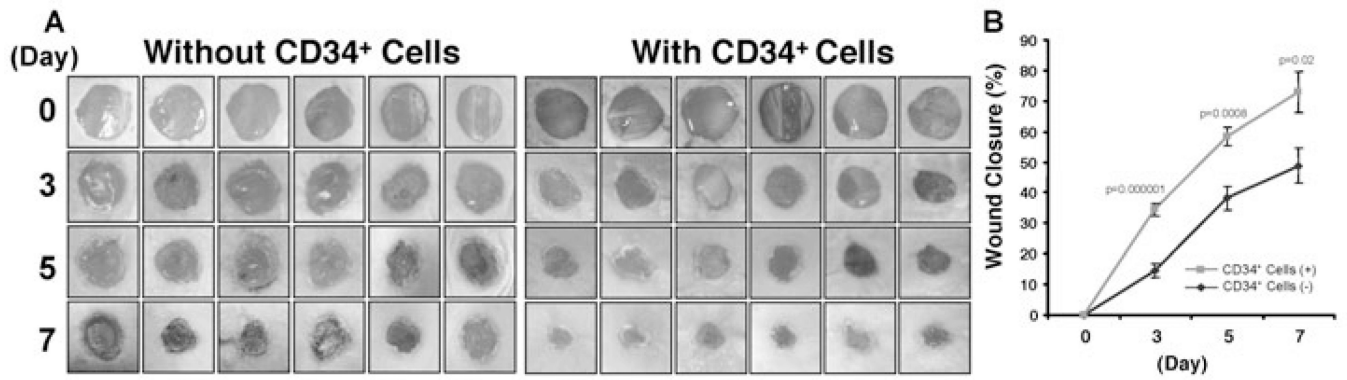


**Figure 7. CD34<sup>+</sup> cells secrete collagen**

Total soluble collagen was measured by using a Sircol Collagen Assay kit from the culture supernatants of CD34<sup>+</sup> cells after 24 h and 48 h of fasting, compared with baseline values, and graphically presented. Results are shown as mean ± SEM (n=3) within a representative of three independent experiments.

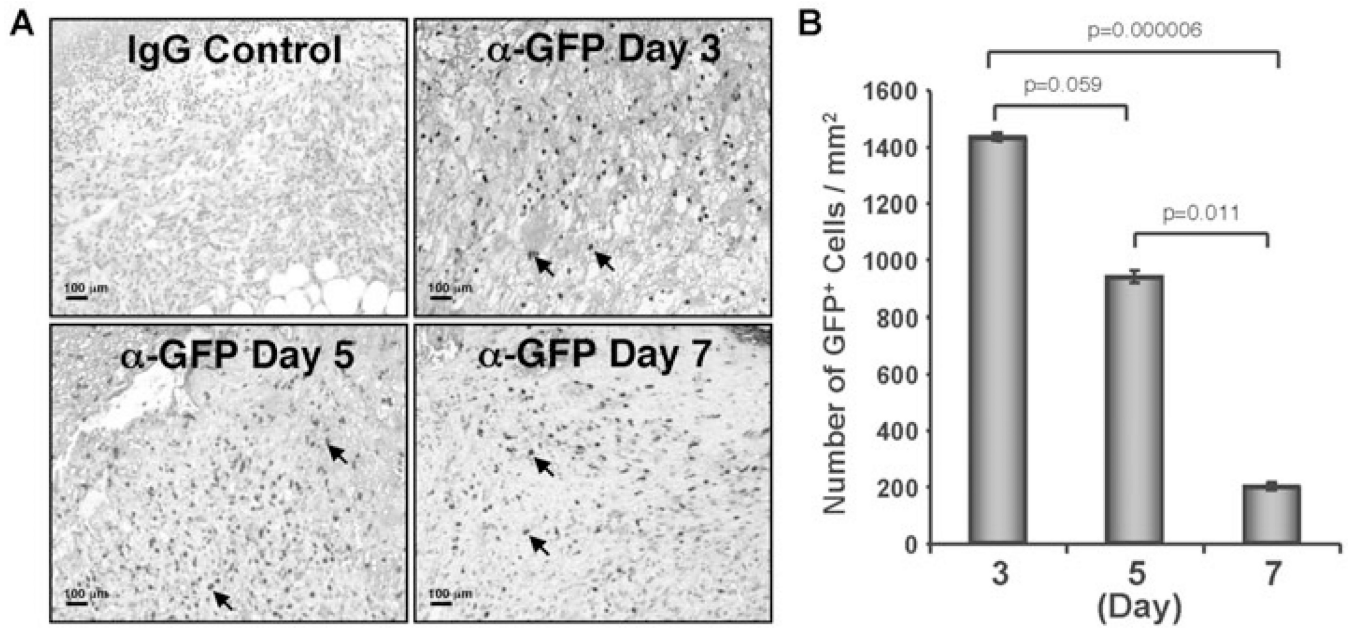


**Figure 8. CD34<sup>+</sup> cells enhance expression of collagen 1A1 and reduce expression of MMP1**

**A.** Graphical presentation of real-time PCR analysis data of collagen 1A1 (COL1A1, left, upper panel) and MMP1 (left, lower panel) gene expressions in cultured human primary dermal fibroblasts in presence or absence of CD34<sup>+</sup> cells at various time points. Similar experiments were performed for expression of COL1A1 (right, upper panel) and MMP1 (right, lower panel) genes in fibroblast cells in presence or absence of proteasome inhibitor (MG132). Internal house keeping gene  $\beta$ -actin was used as a reference for normalization. Data expressed as  $\pm$  SEM (n=3 in triplicate). The expression level of each target gene in fibroblast without any treatment was considered as base line. **B.** Western blot analysis was performed for C-Jun in human primary dermal fibroblast cells cultured in presence or absence of CD34<sup>+</sup> cells (1:1 ratio and CD34<sup>+</sup> cells were removed after culture) plus presence or absence of proteasome inhibitor (MG132) and JNK inhibitor II (SP600125) at various time points. GAPDH protein was evaluated as a house keeping control. Quantitative values of C-Jun were calculated by performing densitometric analysis of the targeted protein bands and graphically presented relative to GAPDH amount. Results are shown as mean  $\pm$  SEM (n=3) within a representative of three independent experiments.